# We are IntechOpen, the world's leading publisher of Open Access books Built by scientists, for scientists

6,900
Open access books available

186,000
International authors and editors

200M
Downloads

Our authors are among the

154
Countries delivered to

TOP 1%
most cited scientists

12.2%
Contributors from top 500 universities


WEB OF SCIENCE™

Selection of our books indexed in the Book Citation Index in Web of Science™ Core Collection (BKCI)

## Interested in publishing with us?
## Contact book.department@intechopen.com

Numbers displayed above are based on latest data collected.
For more information visit www.intechopen.com

Chapter 11

# Controlled Rate Thermal Analysis (CRTA) as New Method to Control the Specific Surface in Hydroxyapatite Thin Coatings

E. Peón, A. El hadad, F.R. García-Galván,
A. Jiménez-Morales and J.C. Galván

Additional information is available at the end of the chapter

http://dx.doi.org/10.5772/66468

**Abstract**

The control of the texture in synthetic hydroxyapatite ceramics had limited their application in the field of the materials for bone implantation, even more when it is used as a filling in cements and other formulations in orthopedic surgery. The present article shows preliminary results demonstrating the effectiveness of a modification of the controlled rate thermal analysis (CRTA), developed by J. Rouquerol, used for the preparation of ceramic materials with controlled textural characteristics, during the formation of ceramic powders of synthetic hydroxyapatite at low temperatures. The thermal treatments of the hydroxyapatite were carried out in a device connected to a computer, to control temperature and pressure system, keeping the decomposition speed constant. Results, reported when preparing ceramic powders of hydroxyapatite at 300 and 850°C under controlled pressure, using synthetic hydroxyapatite with a Ca/P molar ratio equal to 1.64, were checked using IR spectroscopy and X-ray diffraction, showed that the formed phase corresponds to that of crystalline hydroxyapatite, even at 300°C of maximum temperature. Values of specific surface (BET) between 17 and 66 $m^2/g$, with pore size in the range of 50–300 Å in both cases are obtained by $N_2$ absorption isotherms, when analyzing the isotherms of nitrogen absorption.

**Keywords:** hydroxyapatite, formation, thermal analysis to controlled speed, specific surface, pore size

INTECH
open science | open minds

© 2017 The Author(s). Licensee InTech. This chapter is distributed under the terms of the Creative Commons Attribution License (http://creativecommons.org/licenses/by/3.0), which permits unrestricted use, distribution, and reproduction in any medium, provided the original work is properly cited. CC BY

## 1. Introduction

It is known the diversity of materials in use today as bone substitutes. Among them the hydroxyapatite (HA) has deserved special attention because of its excellent biocompatibility, almost the same of that of natural bone. Most of commercial HA used in clinical and research applications are in solid and granulated forms with pore sizes between 100 and 150 μm. It has been demonstrated that such a range of pore dimension is appropriate to cause tissue growth in direct applications as bone substitutes [1–5]. HA ceramics and thin films can be synthesized by many methods [3, 4]. The conventional chemical precipitation method is the more extended method [6]. Following chemical precipitation, combination methods and the hydrothermal process are the next most well-known methods of preparing HA [6–10]. Nevertheless, the scientific community is devoting great efforts looking for new alternative methods in order to obtain hydroxyapatite ceramics with improved microstructural and corrosion properties. In this way, laser-assisted bioprinting and pulsed laser deposition techniques are very promising methods to obtain this kind of hydroxyapatite ceramics and thin films [11–14]. Also, alternating current electric field modified synthesis [15] and magnetron sputtering techniques (MST) [16, 17].

In this context, several methods of synthesis of HA with appropriately controlled textural characteristics as well as its use as a filler in formulations for systems in orthopedic surgery have been reported, however, the uniformity of the pore size is a problem unsolved up to now [18–20]. The sol-gel synthesis of HA thin films and ceramics has attracted much attention because it offers a molecular-level mixing of the calcium and phosphorus precursors, which is capable of improving chemical homogeneity of the resulting HA to a significant extent, in comparison with conventional methods [18–20]. Fortunately, Vila et al. have obtained significant progress in recent years using the sol-gel process [22]. In the context of the present work, they have obtained a bimodal porous process for nanocrystalline hydroxyapatite (HA) coatings with pore sizes in the range of meso/macrometer scale deposited onto Ti6Al4V substrates by the sol-gel method using nonionic surfactants as the porous former agent [22].

When phosphates are treated at several temperatures important changes occur in their properties, in particular, in their chemical contents and physicochemical characteristics, which permit an assessment of admixtures in the phosphates and the effects of substitution of the fundamental elements with others. But, on the other hand, the thermal treatment of the material poses a serious problem, due to difficulties to effectively control the gradients of pressure and temperature originated in different parts of the sample in most experiments [23–25].

The method for the thermal analysis developed by Rouquerol [26, 27], known as “control rate thermal analysis” (CRTA), has been tested in formulations for the control of textures in solids [28–30]. This method is very useful in cases of complex thermolysis usually lapses through superimposed, parallel or serial reactions. Thermal treatment at a controlled speed can allow the formation of homogeneous porosity and a homogeneous surface in its chemical composition and distribution of defects.

http://dx.doi.org/10.5772/66468

In previous studies, we have prepared organic-inorganic hybrid sol-gel films with nanocrystalline hydroxyapatite as a filler and triethylphosphite (TEP)as a network forming agent to enhance the *in vitro* biocompatibility and corrosion protection of these coatings deposited on Ti6Al4V alloys [31, 32]. Now, the purpose of this new study is to apply the CRTA technique to crystallize synthetic HA with a controlled specific surface and homogeneous distribution of pores, appropriate to be used in bone implantation and other formulations for orthopedic surgery. These parameters may be very important in different situations. For example, when HA is used as a filler in cement-based composites, the superficial specific area must be small because a frail material may be obtained due to the presence of microfracture centers when are too big. Taking into account thermogravimetric analysis results, several pressures and temperatures of control were tested in the preparation of ceramic powders.

## 2. Experimental

### 2.1. Preparation of hydroxyapatite

Hydroxyapatite used in this study was obtained by hydrolysis and condensation of suitable precursors following a water-based sol-gel process in accordance with the preparation method of Dean Mo Liu et al. [33–35]. Triethylphosphite (TEP), $C_6H_{15}O_3P$ (Aldrich, 98%) and calcium nitrate tetrahydrate, $Ca(NO_3)_2{\cdot}4H_2O$ (Aldrich) were used as precursors of phosphorus and calcium, respectively.

The preparation process includes the following stages: the first stage is the hydrolysis of the precursor of phosphorus. TEP is mixed with ultrapure distilled water under vigorous agitation. Given the immiscibility between TEP and water, the mixture initially becomes opaque. However, after 24 hours of agitation the emulsion is transformed into a clear dissolution indicating that the TEP is hydrolyzed completely. In the second stage, the saline precursor of calcium is added to the medium in a stoichiometric quantity (Ca/P molar ratio = 1.64) using a 4 M aqueous solution of nitrate of calcium. In this step, the agitation is continued for 30 min and then the mixture is left to stand for 24 hours at room temperature. The gelation is guaranteed by the evaporation of the solvent at 80°C, until a viscous liquid is obtained whose volume is about 40% of the initial solution.

### 2.2. Preparation of HA sol-gel coatings on Ti6Al4V substrates

Ti6Al4V disks of 2 cm of diameter and 0.4 cm of thickness were polished using different silicon carbide grit up to 1200 grade. The substrates were ultrasonically degreased with acetone for 10 min and washed with distilled water. Finally, the substrates were dried at 200°C for one hour in an air oven to form a titanium oxide layer. The formation of $TiO_2$ layer might decrease the stress concentration and thermal expansion coefficient mismatch between the coatings and the titanium substrate.

These substrates were dip coated in the HA sol solution, with a dipping and withdraw speed of 12 cm/min. The sol-coated substrates were then immediately transferred into an air oven and held at 80°C for 30 min to stabilize the deposited layer. To increase the coating thick-

ness, the above process was repeated three times and finally it was thermally treated under conventional and controlled rate thermal treatments (CRTA). Cross section SEM micrographs revealed that the estimated thickness of all the HA crystalline sol-gel derived coatings was about 1–2 μm. Nevertheless, these thicknesses were nonuniform due to roughness of the Ti6Al4V substrate.

### 2.3. Crystallization of hydroxyapatite under conventional and controlled rate thermal treatment

The conventional thermal treatment was carried out in a furnace, burning the precipitate at various temperatures (600, 800°C) for 2 h, at a heating speed of 2°C/min. For the controlled rate thermal analysis (CRTA), samples of 1 g were placed in a quartz sample holder, which was introduced in a programmable tubular oven with Eurotherm control of ±1°C error temperature and connected to a vacuum group, where a Pirani for measuring pressure and a diaphragm with an aperture of 0.1 mm are already present. A home-made software allows the regulation of the temperature and the measurement of generated pressure. This last parameter is the one that regulates the transformation rate. The basis of this thermal treatment is to control the temperature and the pressure system, keeping the decomposition rate constant. **Figure 1** shows a photograph of the CRTA equipment and a simplified schematic diagram of the device.

In parallel studies a set of HA sol-gel coatings previously deposited on Ti6Al4V substrates was densified at the optimal pressure and temperature, which is determined by CRTA. The adequate pressure was accomplished with the use of a vacuum pump connected to the muffle furnace.

### 2.4. Characterization of the powders of hydroxyapatite

The relation Ca/P was calculated starting from the percentage of Ca, determined by absorption spectroscopy in Philips Pye Unicam SP9 at a $\lambda$ = 422.7 nm and the percentage of P obtained by emission spectrometry in a Perkin Elmer Capture 40 at a $\lambda$ = 213.6 nm. On the other hand, powders were characterized by infrared spectroscopy (IR) in a PHILIPS FTIR PU 9800, using the method of pills of KBr and X-ray diffraction (XRD), in a Philips Pye Unicam PW1710, by the method of powders. The thermogravimetric analysis (TGA) was carried out

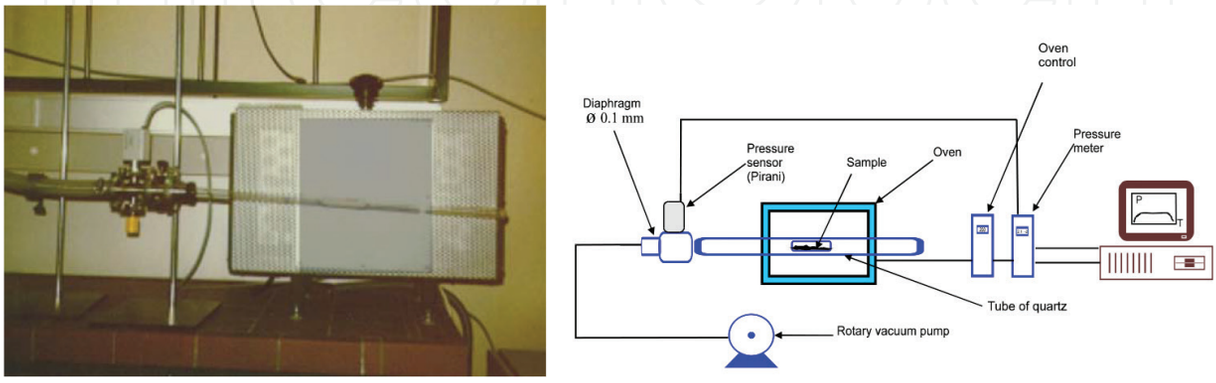


**Figure 1.** Equipment for controlled rate thermal treatment (CRTA).

http://dx.doi.org/10.5772/66468

with 30 mg of the sample in a SHIMATZU at a speed of 10°C/min, up to 1200°C. The morphology of powders was examined by scanning electron microscopy (SEM) in a SEM Tescan Vega TS 5130SB. The specific surface (BET) and porosity of the material were determined in Coulter equipment; model Omnisorp TM 100, starting from isotherms of adsorption for $N_2$ at a temperature of 77 K.

### 2.5. Cytotoxicity/osteoblasts adhesion

The cytocompatibility of coated samples was analyzed by indirect contact as described in ISO 10993-5 (ISO Standards 1999). Briefly, HA coated Ti6Al4V alloy were placed in culture plates and incubated in 15 ml of culture medium (DMEM, Dulbecco's Modified Eagle Medium, Gibco) without fetal bovine serum (FBS) for 24 hours at 37°C. The supernatant of this mixture is called pure extract (100%) which then subjected to dilutions of 0, 10, and 50%.

Fibroblast cells (BALB/c, 3T3, ATCC clone A31) were purchased from American Type Culture Collection (ATCC; MD, USA) and seeded in 24-well plates and cultured in DMEM. 1% antibiotic was added, supplemented with 10% FBS and kept in incubator at 37°C in 5% $CO_2$ atmosphere. The culture medium was then replaced by extracts of the material to which 10% FBS was added and after 24 hours, the cells were counted using a Neubauer camera. The number of cells cultured in DMEM containing 10% FBS alone was considered the negative control (corresponding to 0% of the extract dilution).

The experiment was carried out six times, means and standard deviations were subjected to a variance analysis, considering significant differences if $p < 0.05$. Additionally, were seeded, 30.000 cells of pre osteoblasts of femur of Balb/c 3T3 (FOST) in plates with Ti6Al4V coated samples, these were maintained in culture supplement DMEM with 10% FBS at 37°C and atmosphere of 5% CO2 for 24 hours. At the end of this period, the plates were moved and the cells were fixed in 2.5% of glutaraldehyde solution, then subjected to treatment with 0.1 M of cacodylate buffer solution at pH 7.3 for 24 hours.

After the cells were washed twice with buffer solution 0.1 M cacodylate, dehydrated with increasing concentrations of alcohol (50–100%), they were immersed in ethanol-hexamethyldisilazane absolute solution (50:50 v/v) and then in hexamethyldisilazane (100%) and dried for 24 hours. Finally, metallization of samples with palladium-gold allowed them to be observed using a scanning electron microscope (SEM).

### 2.6. Corrosion behavior

The corrosion behavior of the HA film/Ti6Al4V system was evaluated by applying electrochemical impedance spectroscopy (EIS) [21, 31, 32]. These electrochemical measurements were performed using an AutoLab potentiostat/galvanostat PGSTAT30 equipped with a FRA2 frequency response analyzer module (EcoChemie, The Netherlands). A standard three-electrode cell was used for this purpose. The working electrode was the investigated sample with an area of 3.14 $cm^2$. The reference and the counter-electrode were a saturated calomel electrode (SCE) and a large size graphite sheet, respectively. The electrochemical cell was filled with Kokubo's solution. (SBF; pH = 7.4) [36, 37]. The EIS measurements were made at the open

circuit potential (OCP). Logarithmic frequency scans were carried out by applying sinusoidal wave perturbations of ±10 mV in amplitude, in the range of $10^{5}$–$10^{-3}$Hz. Five impedance sampling points were registered per frequency decade. The impedance data were analyzed by using the ZView software, version 3.5a (Scribner Associates Inc, Southern Pines, NC, USA).

## 3. Results and discussion

### 3.1. Characterization of the powders of hydroxyapatite

The Ca/P rate was determined by chemical analyses (absorption spectroscopy for the Ca and emission spectrometry for the P) of the powder preparations and was 1.64. This rate is appropriate to keep the apatite structure after the thermal treatment.

It has been found reports are scarce in the literature of application of controlled rate thermal treatment (CRTA) technique, for treatments of HA. Consequently, a thermogravimetric analysis (TGA) of as-prepared HA green powders (without a previous thermal treatment) was carried out (**Figure 2**) for determining the characteristic temperatures of HA decomposition. The TGA showed different stages in the thermolysis of HA, the first one is associated with the dehydration. The second one and last one are associated with dehydration-crystallization. These processes have been studied by other authors [38–40]. However, practically no effort has been dedicated to study the influence of the experimental conditions used for the thermal decomposition on the morphology of the final products.

The results obtained for TGA, were verified by CRTA (**Figure 3**) to obtain characteristic temperatures and partial pressure for each step of crystallization of the HA. **Table 1** shows the

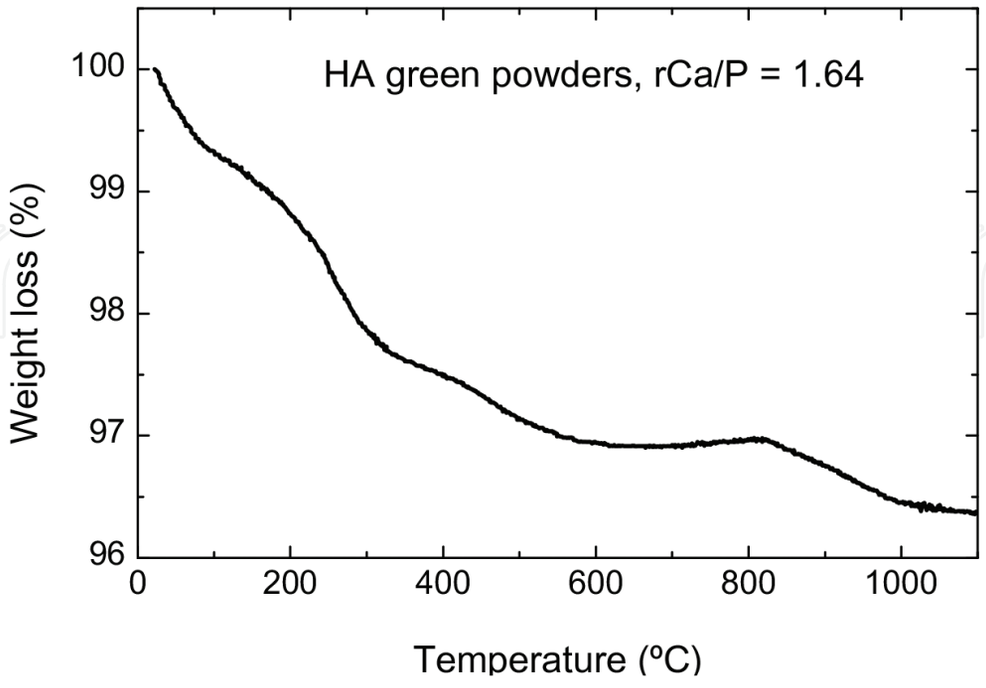


**Figure 2.** TGA of as-prepared HA green powders.

http://dx.doi.org/10.5772/66468

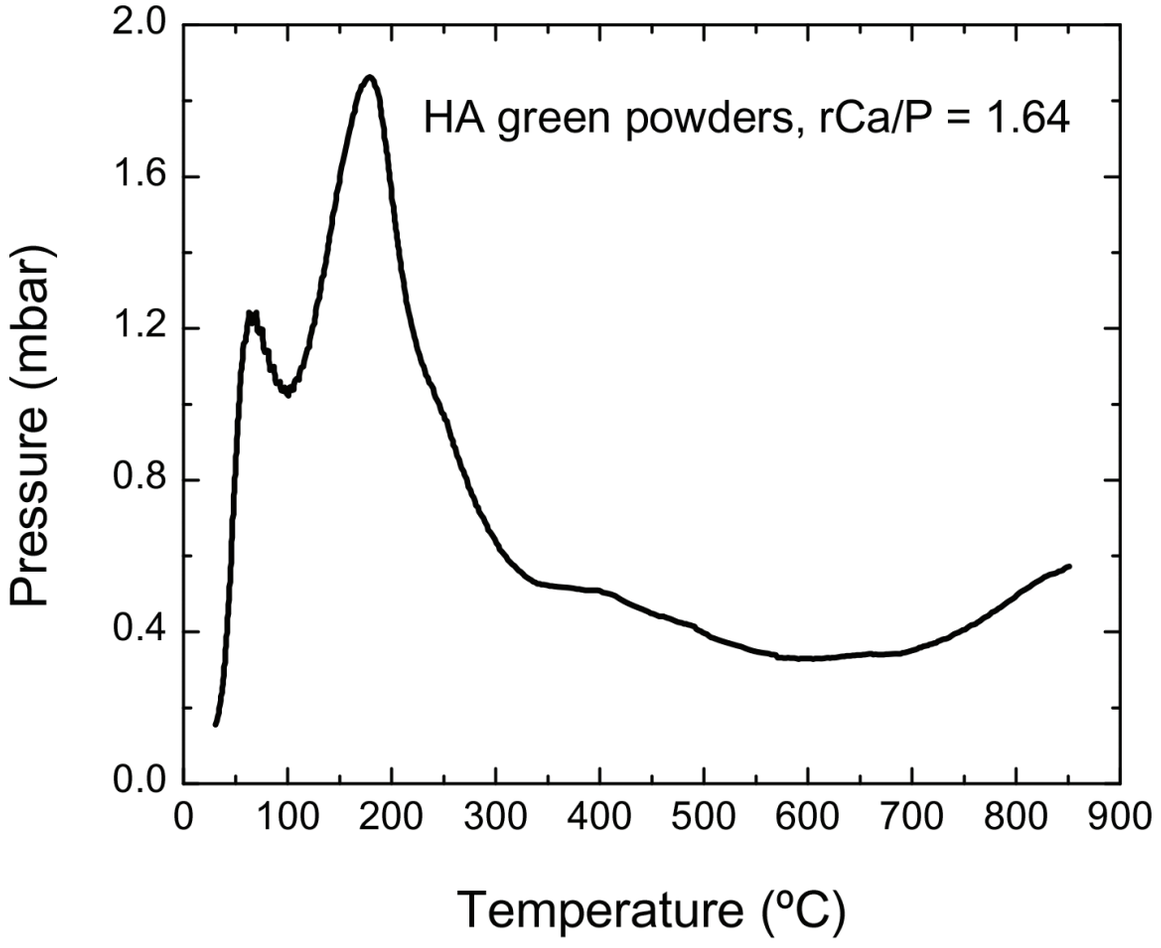


**Figure 3.** CRTA of as-prepared HA green powders.

| Sample | $r_c$ (°C/min) | $T_{cp}$ (°C) | $p_c$ (mbar) | $T_m$ (°C) |
|---|---|---|---|---|
| HA-1 | 2 | 100 | 2.65 | 300 |
| HA-2 | 2 | 100 | 0.50 | 300 |
| HA-3 | 2 | 300 | 1.00 | 850 |
| HA-4 | 2 | 300 | 0.33 | 850 |

**Table 1.** Experimental conditions for the CRTA.

experimental parameters used in the different CRTA, which seeks to determine the optimal parameters of crystallization of HA at the lower temperature; where $r_c$ is the controlled rate, $T_{cp}$ is the temperature of control of the pressure, $p_c$ is the pressure of control and $T_m$ is the maximum temperature used to achieve such pressure control.

Analyses by IR and XRD demonstrated that both types of the sample, conventional treated and treated with CRTA, were pure crystalline phases of HA.

In **Figure 4** are shown the IR spectra typical of HA without thermal treatment (HA-green), conventional thermal treatment (HA-CTT) and after CRTA (HA-1 to HA-4), where the characteristic bands observed are reported for this material type, corresponding to the fundamental vibrations 3571.46 and 631.73 $cm^{-1}$ of the $OH^-$ and $\nu_3$ 1092.75 and 1045.49 $cm^{-1}$, $\nu_1$ 963.51 $cm^{-1}$, $\nu_4$ 602.80 and 568.08 $cm^{-1}$ of the $PO_4^{3-}$ [41].

The bands are very similar in all the IR spectra (**Figure 4**). The wide band from $OH^-$ vibration only could be observed in the green-HA and in HA-CTT and was due to hydrate water

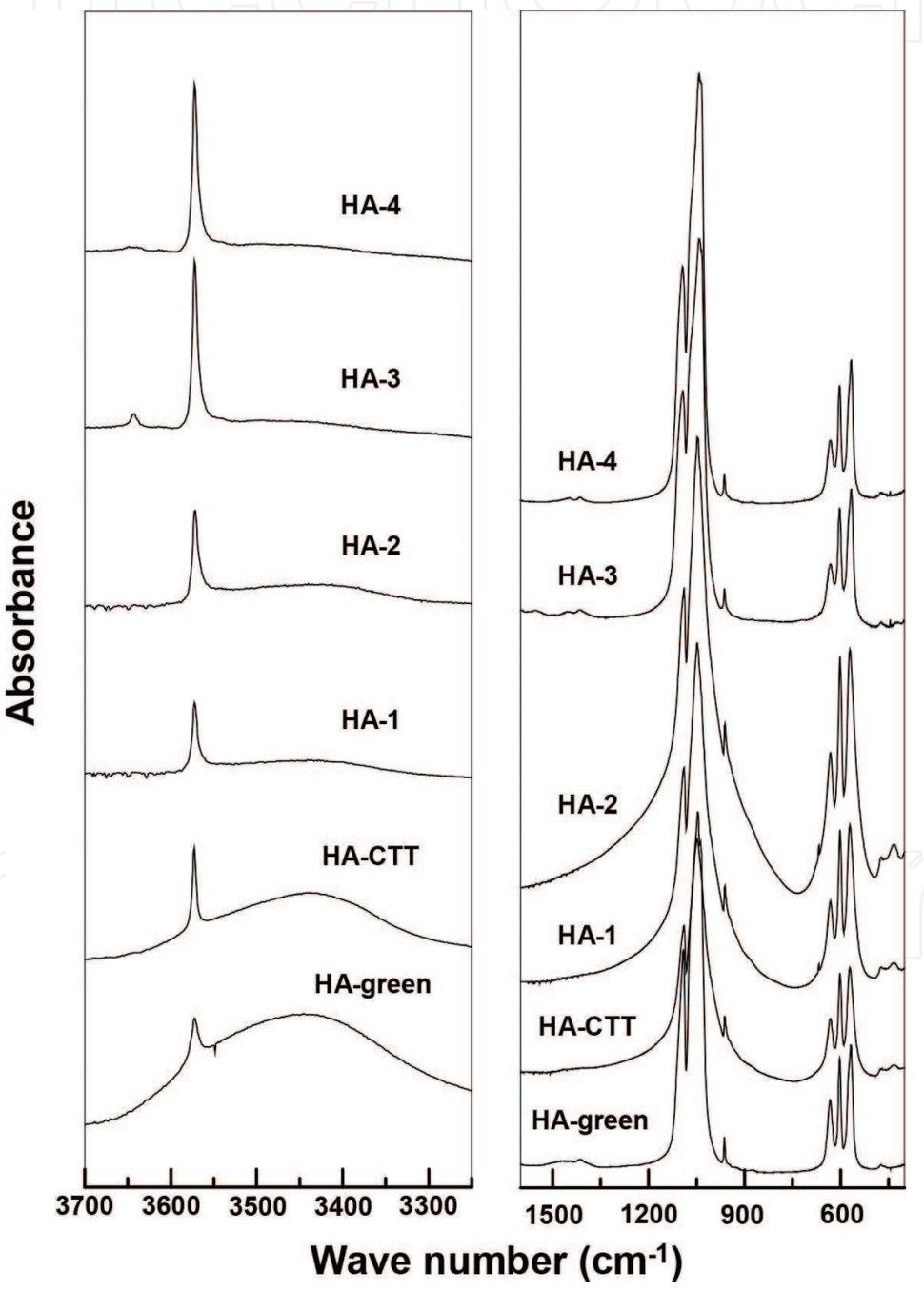


**Figure 4.** FTIR spectrum characteristic of an as-prepared HA-green sample and HA samples after the thermal treatments.

http://dx.doi.org/10.5772/66468

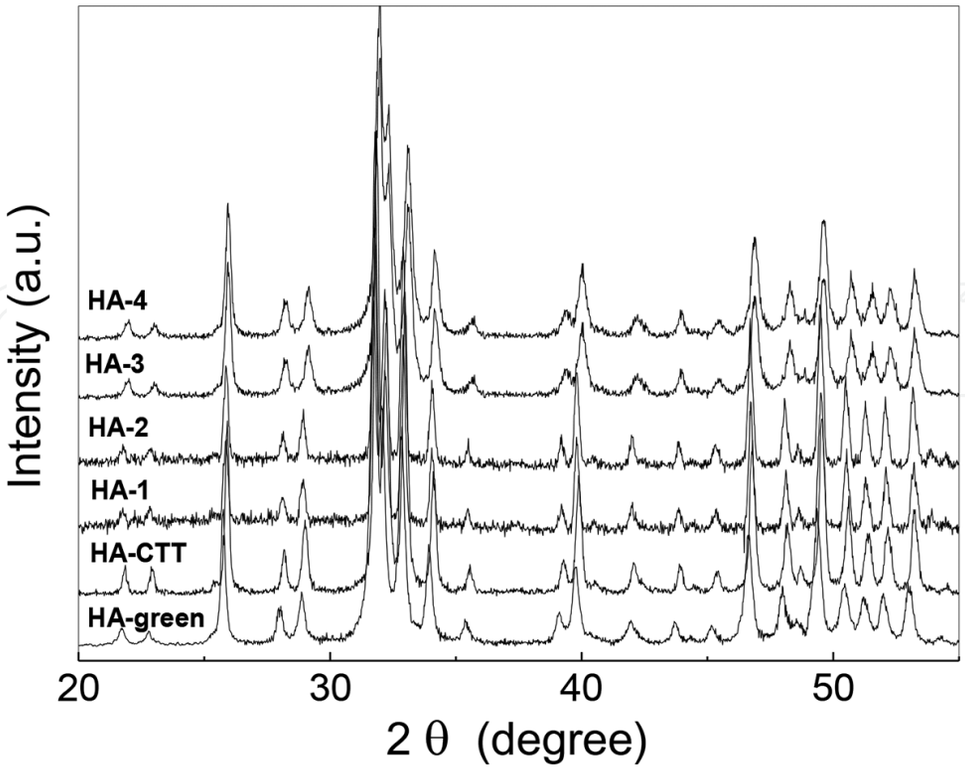


**Figure 5.** X-ray diffraction pattern of as-prepared HA green powders and HA samples obtained by applying different thermal treatments.

(3442.22 $cm^{-1}$). All bands become narrower and more symmetrical for HA-3 and HA-4, indicating an increase in the crystallinity of the material according to results obtained by other authors [42, 43].

**Figure 5** shows X-ray diffraction, where typical lines for this material appear. In all cases, the signs appeared in X-ray diffraction corresponds to those reported in Chart No. 9-432 of ASTM [44, 45].

By applying conventional thermal treatments, HA was typically calcined above 900°C in order to obtain a stoichiometric, apatitic structure. However, it is interesting to note that applying CRTA the degree of crystallization of HA in this study at temperatures as low as 300°C it can be observed in **Figure 6a** and **6b**. The HA here obtained was composed of white tiny crystals, where the particles are fused together and, consequently, they are forming a cluster. This phenomenon might be attributed to a high surface area to volume ratio of ultrafine crystals related to thermal treatments. It should be also pointed out that the shape of HA grains is quite different from the biological apatite, which mostly exhibits a needle-like structure. However, we expect that it may be possible to obtain a grain shape similar to biological apatite by optimizing CRTA conditions.

Results for surface measures by BET method are described in **Table 2**. In the table, the range of specific surface areas achieved after CRTA can be observed. Samples HA-1 and HA-2 showed remarkable dependence on pressure for the surface area, increasing almost to double when

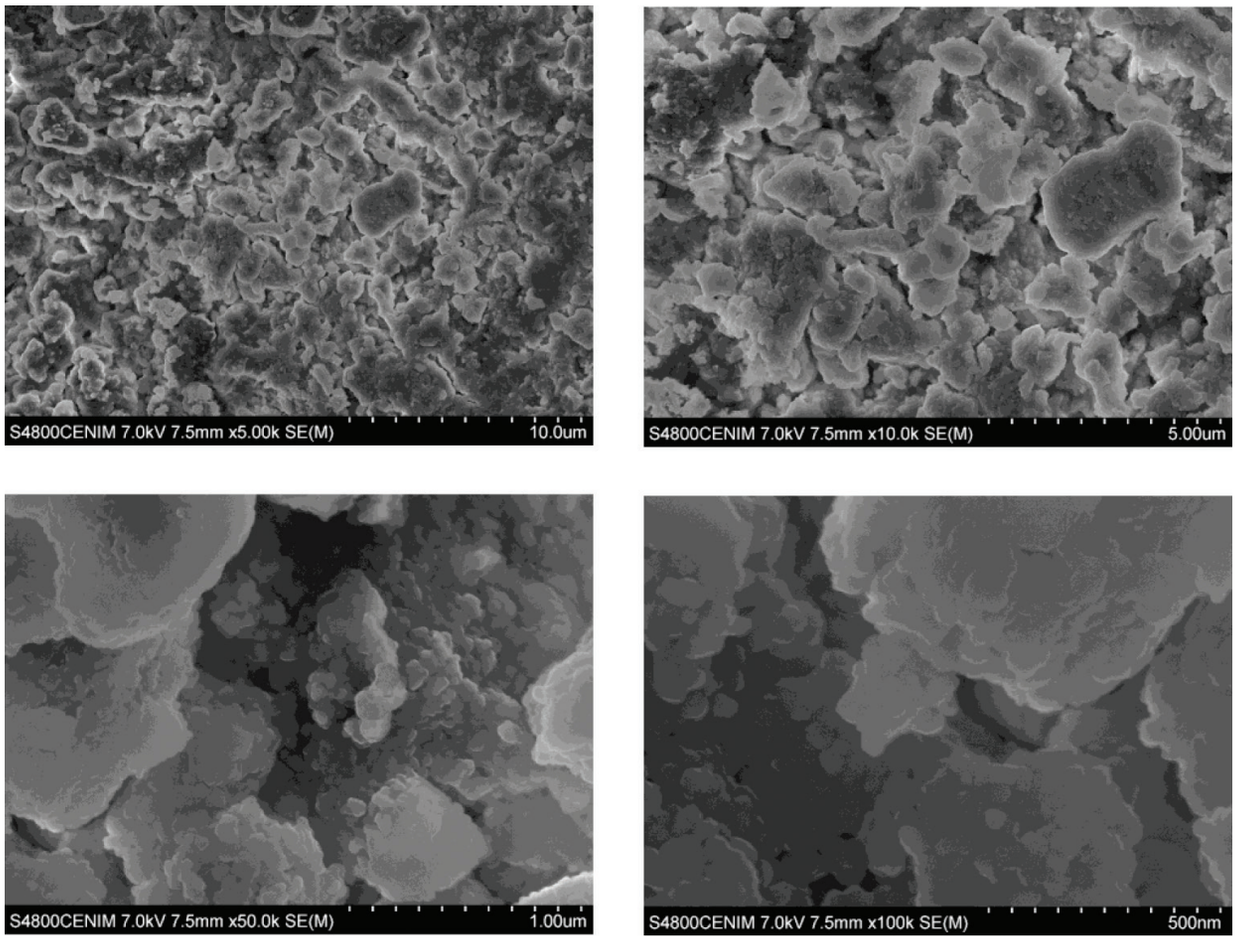


**Figure 6.** SEM micrographs under different magnifications of HA-2 powders prepared using CRTA ($T_m$ = 300°C).

| Sample | S (BET) ($m^2/g$) |
|---|---|
| HA-CTT | 14.0 |
| HA-1 | 34.9 |
| HA-2 | 66.7 |
| HA-3 | 17.2 |
| HA-4 | 26.0 |

**Table 2.** Determinations of the surface area obtained by the BET method for HA-CTT and for different CRTA experimental conditions.

this parameter diminishes, at equal temperature of control and final. It is standing out that both samples, in spite of having been treated at 100°C as the temperature of control for pressure, and at 300°C as the final temperature, crystallized in a pure phase of hydroxyapatite.

In samples HA-3 and HA-4, also the same behavior is also observed, that is to say, an increase of the surface area when diminishing the control pressure, in this case it is four times less.

http://dx.doi.org/10.5772/66468

Although for both samples, the surface area notably diminishes when increasing the temperature of control and the final temperature of the process.

In summary, CRTA technology offers a better resolution and a more detailed interpretation of the decomposition processes of hydroxyapatite via approaching equilibrium conditions of decomposition through the elimination of the slow transfer of heat to the sample as a controlling parameter on the process of decomposition.

### 3.2. Cytotoxicity and adhesion of osteoblasts

The cytotoxicity assay allows toxicological risk assessment of a material by using cell cultures. Taking into account that migrating substances from biomaterials interact at the cellular level with cell membranes, the cellular organelles (mitochondria and Liposomes), the synthesis of proteins and DNA, cell division and the sequence of DNA, this essay covers from the cell

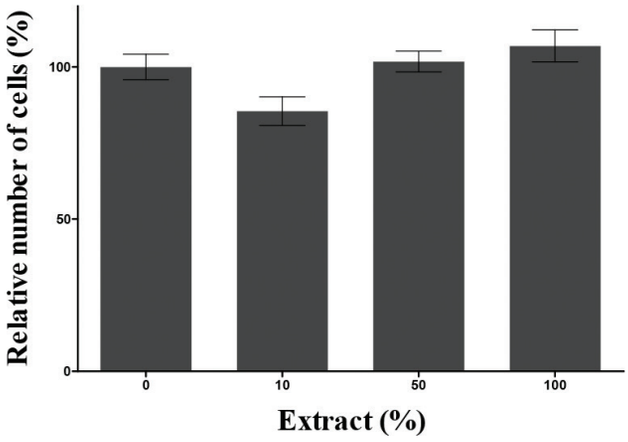


**Figure 7.** Relative number of cells as a function of exposure to different concentrations of extract for a Ti-6Al-4V alloy coated by sol-gel with HA-2 film.

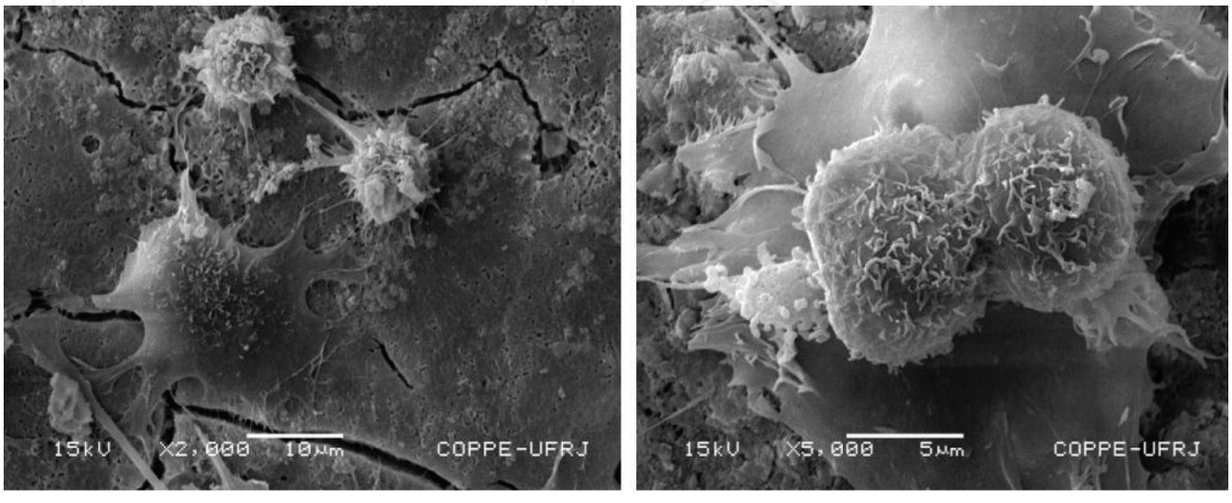


**Figure 8.** SEM images of cells morphology cultured on Ti-6Al-4V sheets coated by sol-gel with HA-2 film.

viability and death to more sophisticated forms that have to do with the cell functionality and genotoxicity.

**Figure 7** shows, the percent (%) of living cells in each one of the tested extracts. The concentration of 0 corresponds to the negative control, or cells without being subjected to any concentration of the extracts.

It can be observed that there is no significant difference ($p > 0.05$) in the number of living cells exposed to different concentrations of the extracts of cultures with alloys coated by HA sol-gel, with respect to the control group. This indicates that HA coatings on Ti6Al4V does not affect the viability of the cells evaluated, which demonstrating its cytocompatibility.

SEM (micrographs) of preosteoblast cells femur seeded in Ti6Al4V alloy coated by sol-gel are shown in **Figure 8**. It is observed that cells were emitting cytoplasmic extensions (filopodia and pseudopodia) that indicate adhesion to the substrate. In addition, mitotic phases were observed (large cells) which suggested that the cells were divided. Apparently, all layers of HA indicate a good biocompatibility because the living cells of osteoblasts hold and spread (propagated) well over all the coating. The observed biocompatibility of HA could be due to roughness and surface porosity that provides sites for attachment and growth of cells.

### 3.3. Corrosion behavior

The corrosion protection behavior of the HA films deposited on Ti6Al4V samples was evaluated by applying electrochemical impedance spectroscopy (EIS). **Figure 9** shows the Bode impedance spectra for the tested samples the in Kokubo's solution at variable immersion time (1 hour and 1, 3, 7, 15 and 30 days).

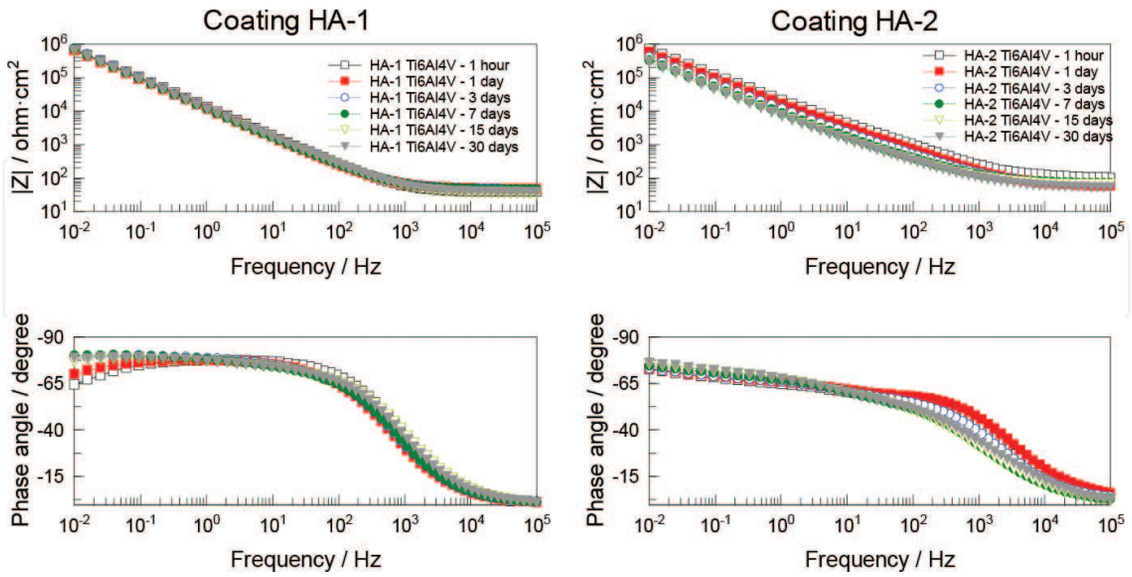


**Figure 9.** Bode impedance spectra representing the evolution of the impedance modulus (|Z|) in a double-logarithmic scale and the phase angle in a semi-logarithmic scale versus frequency for Ti6Al4V/HA coating systems at different immersion time in Kokubo's solution. Coatings: HA-1 and HA-2.

http://dx.doi.org/10.5772/66468

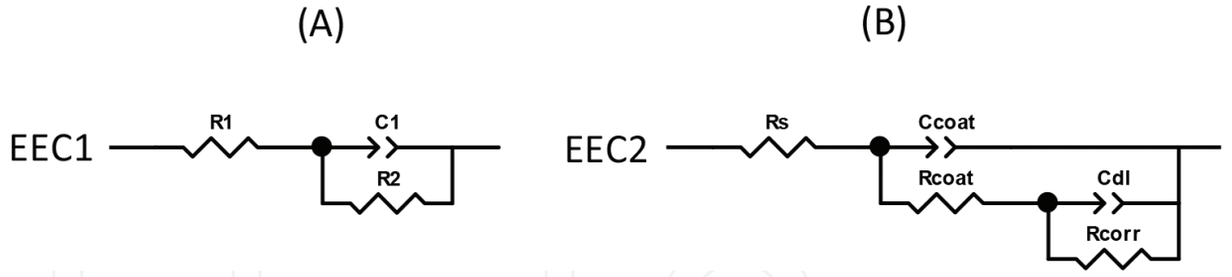


**Figure 10.** Electrical equivalent circuits used for studying the corrosion behaviour of the Ti6Al4V/hydroxyapatite coating system in contact with Kokubo's solution. One time-constant circuit (A) and two time-constant circuit (B).

In these Bode plots, the modulus of the impedance |Z| and the phase angle are represented versus the frequency, the first one in double-logarithmic scale and the second in semi-logarithmic scale.

These impedance spectra can be ascribed to the typical behavior of porous thin films deposited on metal substrates with high corrosion resistance [21, 31, 32, 46, 47]. In the first approach, the single electrical equivalent circuit EEC1 shown in **Figure 10a** can be used to describe the electrochemical behavior of these systems. $R_s$ is associated with the resistance of the electrolyte sited between the working electrode and the reference electrode. The problem is to assign a correct physical meaning to the elements *C*1 and *R*2. Respectively, *C*1 could be associated with the coating capacitance or to the double layer capacitance at the base of the pores filled with electrolyte into the thin film. *R*2 could be ascribed the ionic resistance of the coating pores impregnated with electrolyte or to charge transfer of the metal/electrolyte interface at the base of the pores. In some cases, the electrical equivalent circuit EEC2 shown in **Figure 10b** could be more convenient to describe the impedance plots of these metal/coating systems [48, 49]. Following the notation of the ZView software [49], $R_s$ is the solution resistance of the bulk electrolyte. $C_{coat}$ is the capacitance of the coating. In this case $C_{coat}$ is implemented as a constant phase element (CPE). $R_{coat}$ is the resistance of the coating and $C_{dl}$ represents the double layer capacitance of the electrolyte/metal surface interface. This capacitance is also implemented as a CPE.

As a representative example, **Figure 11** shows fit results obtained by using these two electrical equivalent circuits and complex nonlinear least-squares (CNLS) analysis methods. Three types of impedance plots are given in **Figure 11**, i.e.; Nyquist plot (for real and imaginary values of IZI), Bode plot (for IZI versus applied frequency) and the other Bode plot (for the phase angle versus frequency). This example corresponds to the Ti6Al4V/hydroxyapatite system based on the HA-1 coating after 1 hour in contact with Kokubo's solution. The fit plots generated by the EEC1 and EEC2 electrical equivalent circuits proposed are good. Physical meaning of the values of the electrical elements of the corresponding equivalent circuit and relative errors in % are also good. Finally, the chi-squared values ($\chi^2$) are also very acceptable ($9.9 \times 10^{-4}$ for EEC1 and $3.9 \times 10^{-4}$ for EEC2). It is known that low values of $\chi^2$ are related to a better quality of the fitting results [31, 32].

However due to the uncertainty associated with the difficult interpretation of the results generated by these adjustments and simulations, has been more useful to follow the variations of

the impedance modulus |Z| at the lowest frequency as a function of exposure time of coatings to the Kokubo's solution. This parameter has allowed to reevaluate systematically the results obtained with the impedance measurement.

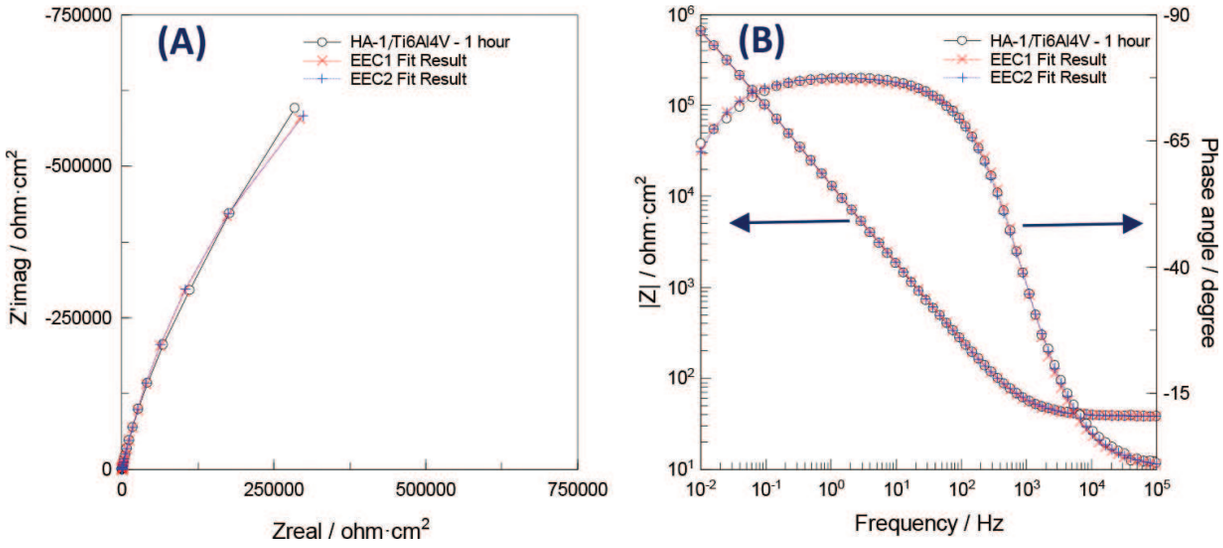


**Figure 11.** Nyquist plots (A), Bode Impedance spectra (B) and fit results obtained by applying the EEC1 and EEC2 electrical equivalent circuits to a Ti6Al4V/hydroxyapatite system based on the HA-1 coating after 1 hour in contact with Kokubo's solution.

**Table 3** shows the variations of the impedance modulus |Z| at a frequency of 10 mHz with the immersion time for Ti6Al4V/hydroxyapatite systems based on the coatings HA-1 and HA-2, respectively. It can observe from the evolution of the values of the parameter $|Z|_{10mHz}$ that both systems show a satisfactory stability when they are tested in a saline solution. Particularly attractive was the protective behavior of the HA-1 coating whose $|Z|_{10mHz}$ values remained almost constant during the 30 days of the immersion test. However, for the system based on the HA-2 coating, although very slowly the values of this parameter decrease, down

| Immersion time | $\|Z\|_{10mHz}$ (ohm/cm²) | |
|---|---|---|
| | Coating HA-1 | Coating HA-2 |
| 1 hour | $6.60 \times 10^5$ | $7.14 \times 10^5$ |
| 1 day | $6.23\ 10^5$ | $5.74 \times 10^5$ |
| 3 days | $7.31 \times 10^5$ | $4.10 \times 10^5$ |
| 7 days | $7.00 \times 10^5$ | $3.26 \times 10^5$ |
| 15 days | $6.07 \times 10^5$ | $2.97 \times 10^5$ |
| 30 days | $6.54 \times 10^5$ | $2.88 \times 10^5$ |

**Table 3.** Variations of the impedance modulus |Z| for 10 MHz frequency with the immersion time for coatings based on the samples HA-1 and HA-2, respectively.

http://dx.doi.org/10.5772/66468

from 7.14 × $10^5$ ohm/$cm^2$ at the start to 2.88 × $10^5$ ohm/$cm^2$ at the end of the immersion test (30 days). This behavior can be ascribed to a slow loss of the protection properties of the coating HA-2 due to the ingress of electrolyte in the coating pores. These results are indicating that the increase of the control pressure of the CRTA associated with the decrease in specific surface (BET) produces an enhancment of the corrosion protection behavior of the hydroxyapatite coatings. This means that a high specific surface is good for enhancing the adhesion of the preosteoblast cells but provokes a decrease in the corrosion protection of the HA coatings. It is necessary to reach a compromise to balance both properties.

## 4. Conclusion

In the present work, it was demonstrated the effectiveness and usefulness of the CRTA technique, for the preparation of crystallization of powders of synthetic hydroxyapatite and thin films with different specific surface areas, making this technique attractive for medical purposes. The purity of the phase of the samples obtained by CRTA was proved by IR spectroscopy and XRD. Several temperatures of control for pressure and watchword pressures were tested, observing the dependence of the specific surface area to these parameters, making possible to obtain surface areas from 14 up to 66 $m^2$/g. It was possible to crystallize pure hydroxyapatite at temperature of 100°C of control of the pressure and 300°C as maximum temperature. Moreover, the results of this study have also indicated that it was also possible to cover commercial Ti6Al4V alloy with these sol-gel-derived hydroxyapatite thin films. Cytotoxicity tests and corrosion studies showed an improvement for coated surfaces compared to the base Ti6Al4V alloy. Biocompatibility expressed in terms of adhesion of living cells and their spread on coating was also adequate. According to the ISO 10993-5 standard, the system was considered nontoxic. The cytocompatibility test shows that the sol-gel coating did not provoke the cell death significantly higher than the control ($p > 0.05$). In addition, the electrochemical impedance spectra confirm that these sol-gel coatings show promising corrosion protection properties. It can conclude that the sol-gel process in conjunction with the CRTA method can be a viable alternative for the production of crystallized synthetic hydroxyapatite thin films and ceramics with controlled specific surface and homogeneous distribution of pores, appropriate to be used in bone implantation and other formulations for orthopedic surgery.

## Acknowledgements

This work has been supported by the National Program for Materials, Spanish Ministry of Science and Innovation (Project MAT2012-38541-C02-02) and by the Spanish Agency for International Development Cooperation (AECI) under the expert fund project entitled "Development of calcium phosphate ceramics for medical use". SEM images of cells were carried out in COPPE UFRJ.

## Author details

E. Peón[1, 2], A. El hadad[1, 3], F.R. García-Galván[1], A. Jiménez-Morales[4] and J.C. Galván[1]*

*Address all correspondence to: jcgalvan@cenim.csic.es

1 National Center for Metallurgical Research (CENIM), CSIC, Madrid, Spain

2 Center for Biomaterials, Havana University, Havana, Cuba

3 Department of Physics, Al-Azhar University, Cairo, Egypt

4 Universidad Carlos III de Madrid, Avda, Leganés, Madrid, Spain

## References

[1] M. Jarcho, "Calcium phosphate ceramics as hard tissue prosthetics", *Clinical Orthopaedic*, Vol. 157, pp. 259–278, 1981.

[2] K. De Groot, *Bioceramics of Calcium Phosphate*, CDC Press, Inc. Boca Raton, FL, 1983.

[3] J. Black, *Orthopaedic Biomaterials in Research and Practice*, Churchill Livingstone Ed., New York, 1988.

[4] J. B. Park, D. Joseph (Eds.), *Biomaterials*: *Principles and Applications*, CRC Press, Bronzino, 2003.

[5] K. I. Humear, A. D. Séller, R. G. Slighter, S. S. Rothstein, H. P. Drobeck, "Tissue response in dogs to dense HA implantation in the femur", *Journal Oral Maxillofacial Surgery,* Vol. 44, pp. 618–627, 1986.

[6] M. Sadat-Shojai, M. T Khorasani, E. Dinpanah-Khoshdargi, A. Jamshidi, "Synthesis methods for nanosized hydroxyapatite with diverse structures", *Acta Biomaterialia*, Vol. 9, Iss. 8, pp. 7591–7621, 2013.

[7] A. Kumar Nayak, "Hydroxyapatite synthesis methodologies: An overview", *Journal of ChemTech Research*, Vol. 2, Iss. 2, pp. 903–907, 2010.

[8] F. Sun, H. Zhou, J. Lee, "Various preparation methods of highly porous hydroxyapatite/polymer nanoscale biocomposites for bone regeneration", *Acta Biomaterialia*, Vol. 7, Iss. 11, pp. 3813–3828, 2011.

[9] N. Farahiyah Mohammad, R. Othman Fei Yee-Yeoh, "Nanoporous hydroxyapatite preparation methods for drug delivery applications", *Reviews on Advanced Materials Science*, Vol. 38, pp. 138–147, 2014.

[10] A. Shavandi, A. El-Din, A. Bekhit, Z. Fa Sun, A. Ali, "A review of synthesis methods, properties and use of hydroxyapatite as a substitute of bone", *Journal of Biomimetics, Biomaterials and Biomedical Engineering*, Vol. 25, pp. 98–117, 2015.

[11] S. Catros, J. C. Fricain, B. Guillotin, B. Pippenger, R. Bareille, M. Remy, E. Lebraud, B. Desbat, J. Amédée, F Guillemot, "Laser-assisted bioprinting for creating on-demand patterns of human osteoprogenitor cells and nano-hydroxyapatite" *Biofabrication*, Vol. 3, Iss 2, p. 025001, 2011.

[12] K. Mensah-Darkwa, R. K. Gupta, D. Kumar, "Fabrication and characterization of hydroxyapatite-magnesium composite thin films on magnesium plates for implant applications", *ASME International Mechanical Engineering Congress and Exposition, Proceedings (IMECE)*, Vol. 3, Iss. Parts A, B, and C, pp. 717–722, 2012.

[13] K. Mensah-Darkwa, R.K. Gupta, D. Kumar, "Mechanical and corrosion properties of magnesium-hydroxyapatite (Mg-HA) composite thin films", *Journal of Materials Science & Technology*, Vol. 29, Iss. 9, pp. 788–794, 2013.

[14] M. A. Surmeneva, E. A. Chudinova, I. Y. Grubova, O. S. Korneva, I. A. Shulepov, A.D. Teresov, N. N. Koval, J. D. Mayer, C. Oehr, R. A. Surmenev, "Effect of pulsed electron beam treatment on the physico-mechanical properties of hydroxyapatite-coated titanium", *Ceramics International*, Vol. 42, Iss. 1, pp. 1470–1475, 2016.

[15] Z. Janićijević, M. J. Lukić, L. Veselinović, "Alternating current electric field modified synthesis of hydroxyapatite bioceramics", *Materials & Design*, Vol. 109, pp. 511–519, 2016.

[16] V. Nelea, C. Morosanu, M. Iliescu, I. N. Mihailescu, "Hydroxyapatite thin films grown by pulsed laser deposition and radio-frequency magnetron sputtering: Comparative study", *Applied Surface Science*, Vol. 228, Iss. 1–4, pp. 346–356, 2014.

[17] T. Mukhametkaliyev, M. Surmeneva, R. Surmenev, B. K. Mathan, "Hydroxyapatite coating on biodegradable AZ31 and Mg-Ca alloys prepared by RF-magnetron sputtering", *AIP Conference Proceeding,* Vol. 1688, p. 030006, 2015.

[18] S. W. K. Kweha, K. A. Khora, P. Cheang, "The production and characterization of hydroxyapatite (HA) powders", *Journal of Materials Processing Technology*, Vol. 89–90, pp. 373–377, 1999.

[19] S. Madhavi, C. Ferraris, T. J. White, "Synthesis and crystallization of macroporous hydroxyapatite", *Journal of Solid State Chemistry*, Vol. 178, pp. 2838–2845, 2005.

[20] C. Balazsi, F. Weber, Z. Kover, E. Horvath, C. Nemeth, "Preparation of calcium-phosphate bioceramics from natural resources", *Journal of the European Ceramic Society*, Vol. 27, pp. 1601–1606, 2007.

[21] A. A. El Hadad, V. Barranco, A. Jiménez-Morales, E. Peon, J. C. Galván, "Multifunctional sol-gel derived thin film based on nanocrystaline hydroxyapatite powders", *Journal of Physics: Conference Series*, Vol. 252 (1), Art. No. 012007, 2010.

[22] M. Vila, I. Izquierdo-Barba, A. Bourgeois, M. Vallet-Regí, "Bimodal meso/macro porous hydroxyapatite coatings", *Journal of Sol-Gel Science and Technology*, Vol. 57, pp. 109–113, 2011.

[23] C. Balazsi, F. Weber, Z. Kover, E. Horvath, C. Nemeth, "Preparation of calcium-phosphate bioceramics from natural resources", *Journal of the European Ceramic Society*, Vol. 27, pp. 1601–1606, 2007.

[24] D. K. Pattanayak, R. Dash, R. C. Prasad, B. T. Rao, T. R. Rama Mohan, "Synthesis and sintered properties evaluation of calcium phosphate ceramics", *Materials Science and Engineering C*, Vol. 27, pp. 684–690, 2007.

[25] F. Z. Mezahi, H. Oudadesse, A. Harabi, A. Lucas-Girot, Y. Le Gal, H. Chaair, G. Cathelineau, "Dissolution kinetic and structural behaviour of natural hydroxyapatite vs. thermal treatment: Comparison to synthetic hydroxyapatite", *Journal of Thermal Analysis and Calorimetry*, Vol. 95, Iss. 1, pp. 21–29, 2009.

[26] J. Rouquerol, "L'analyse thermique a vitesse de decomposition constant", *Journal of Thermal Analysis*, Vol. 2, Iss. 2, pp. 123–140, 1970.

[27] J. Rouquerol, O. Toft Sørensen, General Introduction to Sample-Controlled Thermal Analysis (SCTA). In: O. Toft Sørensen and J. Rouquerol editors. *Hot Topics in Thermal Analysis and Calorimetry - Sample Controlled Thermal Analysis. Origin, Goals, Multiple Forms, Applications and Future*. Dordrecht: Kluwer Academic Publishers, Vol. 3, pp 1–7, 2003.

[28] K. Nahdi, F. Rouquerol, M. T. Ayadi, $Mg(OH)_2$ dehydroxylation: A kinetic study by controlled rate thermal analysis (CRTA), *Solid State Sciences*, Vol. 11, pp. 1028–1034, 2009.

[29] J. Rouquerol, K.S.W. Sing, P. Llewellyn, Adsorption by Metal Oxides. In F. Rouquerol, J. Rouquerol, K.S.W. Sing, P.L. Llewellyn and G. Maurin editors. *Adsorption by Powders and Porous Solids*, 2nd ed. Amsterdam: Elsevier/AP, pp. 393-465, 2014.

[30] M. D. Alcalá, F. J. Gotor, L. A. Pérez-Maqueda, C. Real, M. J. Dianez, J. M. Criado, "Constant rate thermal analysis (CRTA) as a tool for the synthesis of materials with controlled texture and structure", *Journal of Thermal Analysis and Calorimetry*, Vol. 56, pp. 1447–1452, 1999.

[31] A. A. El hadad, V. Barranco, A. Jiménez-Morales, E. Peón, G. J. Hickman, C. C. Perry, J. C. Galván, "Enhancing in vitro biocompatibility and corrosion protection of organic-inorganic hybrid sol-gel films with nanocrystalline hydroxyapatite", *Journal of Materials Chemistry B*, Vol. 2, pp. 3886–3896, 2014.

[32] A. A. El hadad, V. Barranco, A. Jiménez-Morales, G. J. Hickman, J. C. Galván, C. C. Perry, "Triethylphosphite as a network forming agent enhances in-vitro biocompatibility and corrosion protection of hybrid organic-inorganic sol-gel coatings for Ti6Al4V alloys", *Journal of Materials Chemistry B*, Vol. 2, pp. 7955–7963, 2014.

[33] D. Mo Liu, T. Troczynski, W. J. Tseng, "Water-based sol-gel synthesis of hydroxyapatite: process development", *Biomaterials*, Vol. 22, Iss. 13, pp. 1721–1730, 2001.

[34] D. Mo Liu, Q. Yang, T. Troczynski, "Sol-gel hydroxyapatite coatings on stainless steel substrates", *Biomaterials*, Vol. 23, Iss. 3, pp. 691–698, 2002.

[35] D. Mo Liu, Q. Yang, T. Troczynski, W. J. Tseng, "Structural evolution of sol-gel-derived hydroxyapatite", *Biomaterials*, Vol. 23, Iss. 7, pp. 1679–1687, 2002.

[36] T. Kokubo, H. Kushitani, S. Sakka, T. Kitsugi, T. Yamamuro, "Solutions able to reproduce in vivo surface-structure changes in bioactive glass-ceramic A-W$^{3}$", *Journal of Biomedical Materials Research*, Vol. 24, pp. 721–734, 1990.

[37] T. Kizuki, T. Matsushita, T. Kokubo, "Antibacterial and bioactive calcium titanate layers formed on Ti metal and its alloys", *Journal of Materials Science: Materials in Medicine*, Vol. 25, Iss. 7, pp. 1737–1746, 2014.

[38] A. I. Mitsionis, T. C. Vaimakis, "A calorimetric study of the temperature effect on calcium phosphate precipitation", *Journal of Thermal Analysis and Calorimetry*, Vol. 99, pp. 785–789, 2010.

[39] K. Tõnsuaadu, K. A. Gross, L. Pluduma, M. Veiderma, "A review on the thermal stability of calcium apatites", *Journal of Thermal Analysis and Calorimetry*, Vol. 110, Iss. 2, pp. 647–659, 2012.

[40] K. Tõnsuaadu, M. Peld, V. Bender, "Thermal analysis of apatite structure", *Journal of Thermal Analysis and Calorimetry*, Vol. 72, pp. 363–371, 2003.

[41] B. O. Fowler, "Infrared studies of apatites I", *Inorganic Chemistry*, Vol. 13, pp. 194–206, 1974.

[42] N. Pleshko, A. Boskey, R. Mendelsohn, "Novel infrared spectroscopic method for the determination of crystallinity of hydroxyapatyte minerals", *Biophysical Journal*, Vol. 60, pp. 786–793, 1991.

[43] A. Antonakos, E. Liarokapis, T. Leventouri, "Micro-Raman and FTIR studies of synthetic and natural apatites", *Biomaterials*, Vol. 28, pp. 3043–3054, 2007.

[44] S. Mazumder, B. Mukberjee, "Quantitative determination of amorphous content in bioceramic hydroxyapatite (HA) using x-ray powder diffraction data", *Materials Research Bulletin*, Vol. 30, Iss. 11, pp. 1439–1445, 1995.

[45] E. Landi, A. Tampieri, G. Celotti, S. Sprio, "Densification behavior and mechanisms of synthetic hydroxyapatites", Journal European Ceramic Society, Vol. 20, pp. 2377–2387, 2000.

[46] A. A. El hadad, "An approach to the design new coatings for biomedical applications" [thesis]. Universidad Carlos III de Madrid, Leganés. 2012. Available from: http://e-archivo.uc3m.es/handle/10016/16374 [accessed: 2016-09-19].

[47] E. Peón, "Recubrimientos bioactivos de base hidroxiapatita sobre Ti6Al4V para aplicaciones biomédicas" [thesis]. Universidad de La Habana, Cuba. 2013.

[48] B. Chico, J. C. Galván, D. de la Fuente, M. Morcillo, "Electrochemical impedance spectroscopy study of the effect of curing time on the early barrier properties of silane systems applied on steel substrates", *Progress in Organic Coatings*, Vol. 60, Iss. 1, pp. 45–53, 2007.

[49] ZView 3.5a Software, Scribner Association Inc., D. Johnson. Available from: http://www.scribner.com/ [accessed: 2016-09-19].

IntechOpen

IntechOpen